First-Principles Prediction of Doped Graphane as a High-Temperature Electron-Phonon Superconductor

G. Savini, A. C. Ferrari, F. Giustino

Supplementary Material

DENSITY FUNCTIONAL THEORY CALCULATIONS

Calculations are performed within the framework of density functional theory (DFT) in the local density approximation[1, 2]. The wavefunctions are expanded in a plane-wave basis set with a kinetic energy cutoff of 60Ry[3]. The core-valence interaction is taken into account by using norm-conserving pseudopotentials[4, 5]. We use a $20 \times 20 \times 1$ Monkhorst-Pack[6] sampling of the Brillouin-zone (BZ) for structural relaxations. Energy differences are converged within 5meV/atom. The relaxed lattice parameter is 2.50Å, with a C-C bond length of 1.51Å (similar to the C-C bond length we calculate for diamond, 1.52Å) and a C-H bond length of 1.11Å, in good agreement with previous studies[7, 8]. We use a supercell configuration, with periodic replicas separated by 10Å vacuum in order to minimize interlayer interaction. Phonon modes and EPCs are calculated within density functional perturbation theory (DFPT), as described in Ref.[9]. Phonon frequencies are converged within 2cm^{-1}.

The fractional occupations are described by first-order Hermite-Gaussian smearing[10] and p-doping is simulated using the rigid-band approximation[11]. In this approximation the total valence electrons per carbon atom (Z_C+Z_H=4+1=5**e**) are replaced by $(5-x)$**e** where x is the p-doping concentration (in %). Thus, e.g., 1% p-doping corresponds to one B every 100 C, and the total valence electrons per carbon atom are 4.99 **e**. Figure S1(a) plots the band structures of p-doped graphane within the rigid-band model, compared to a supercell model with substitutional B, Fig. S1(b) plots the corresponding EDOS, and Fig. S1(c,d) the atom-projected EDOS. We use a 2×2 supercell with one B atom, corresponding to 12.5% p-doping (see Fig. S1(e)). In both cases, the doping has the effect of lowering E_F below the top of the valence band, and does not introduce localized states in the band gap. As a result, a small multi-sheet Fermi surface with diameter $2k_F$ (see Fig. S1(a)) emerges around the BZ center. The dispersions close to E_F are essentially identical in the

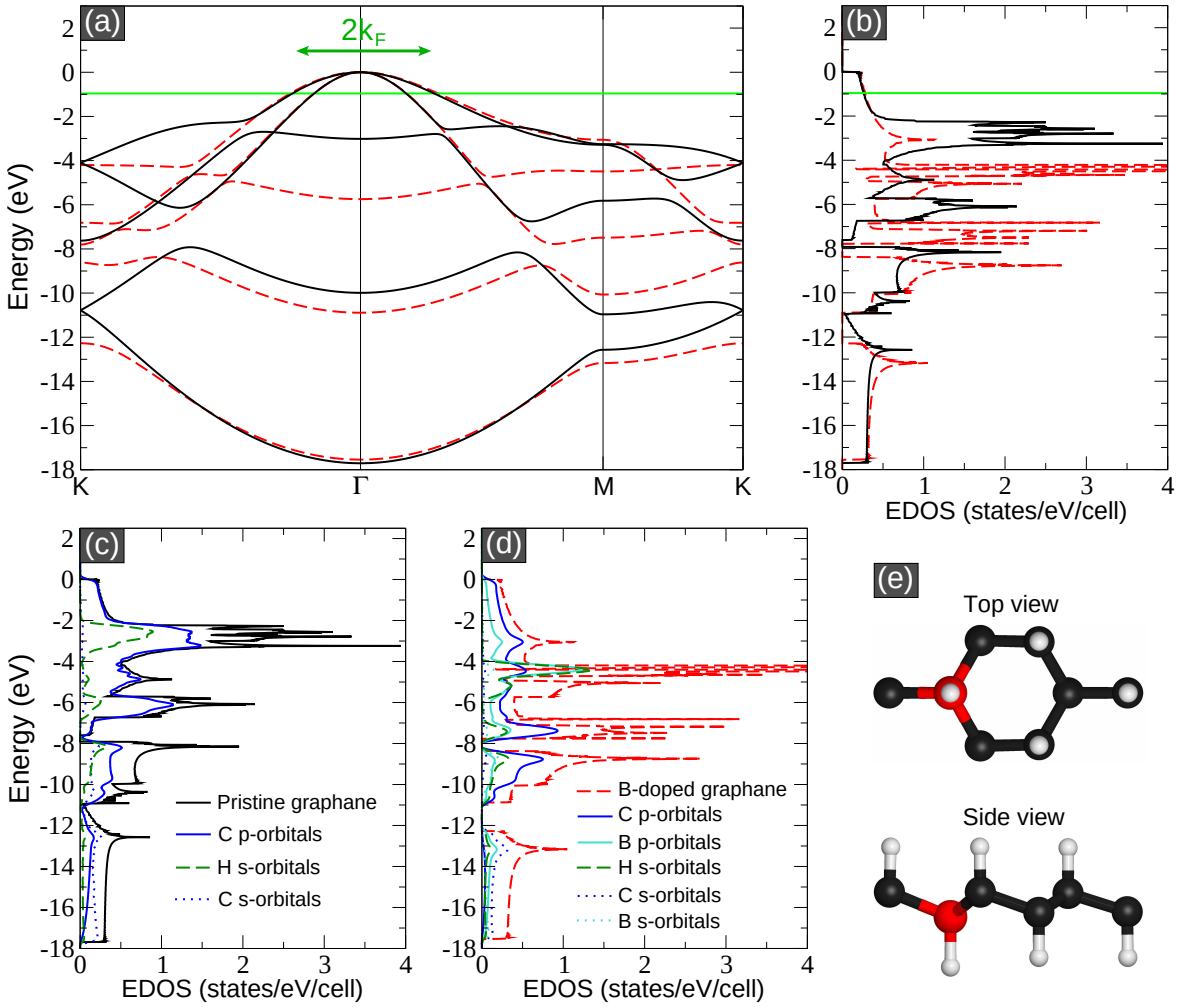

FIG. S1: (a)Band structure of pristine (solid dark lines, rigid band model) and 12.5% p-doped graphane (dashed red lines, 2×2 supercell with B). The top of the valence bands is set to zero, and E_F=-0.96eV (horizontal green line). The arrows indicate the average Fermi surface diameter. (b)EDOS of pristine (solid dark lines) and 12.5% B-doped graphane (dashed red lines). The dispersion close to E_F is similar for the supercell and rigid-band models. We expect this to hold also at lower doping, where the perturbation to the pristine dispersion is smaller. (c)Atom-projected EDOS of pristine graphane. (d)Atom-projected EDOS of 12.5% B-doped graphane. The structure between -2 eV and -4eV in the valence band of pristine graphane is mostly due to the nondispersive H1s states at -2.5eV around $\mathbf{\Gamma}$. Upon doping these are stabilized to $\sim$-4eV by the B atoms positive charge. Other changes in the EDOS reflect the opening of gaps at $\mathbf{K}$, associated with the periodic doping model adopted. (e)Ball-and-stick representations of a 2×2 graphane supercell with one substitutional B (top and side view). C atoms are grey, H white, B red.

Doping	E_F eV	Smearing meV	**k**-mesh	EDOS st./eV/cell	$\Delta\omega$ meV	λ	$\omega_{\log}$ cm^{-1}	T_c K
1%	-0.08	50	$300 \times 300 \times 1$	0.21	58	1.237	708	84.3
2%	-0.18	70	$200 \times 200 \times 1$	0.21	58	1.263	697	85.3
3%	-0.31	120	$120 \times 120 \times 1$	0.22	59	1.314	676	87.0
4%	-0.38	140	$100 \times 100 \times 1$	0.22	59	1.353	660	87.9
5%	-0.47	190	$80 \times 80 \times 1$	0.23	59	1.400	645	89.4
6%	-0.55	220	$80 \times 80 \times 1$	0.24	60	1.422	639	90.2
7%	-0.58	240	$60 \times 60 \times 1$	0.24	60	1.430	637	90.5
8%	-0.73	270	$50 \times 50 \times 1$	0.25	61	1.436	634	90.5
9%	-0.81	270	$50 \times 50 \times 1$	0.26	62	1.446	633	91.0
10%	-0.90	270	$50 \times 50 \times 1$	0.26	64	1.449	632	91.1

TABLE S1: Calculated E_F, EDOS at the Fermi level, phonon softening $\Delta\omega$, λ, logarithmic phonon frequency $\omega_{\log}$ and T_c as a function of p-doping.

the rigid-band and supercell models. The corresponding EDOS at 12.5% p-doping are 0.26 states/eV/cell in rigid-band and 0.27 states/eV/cell in supercell. We expect this similarity to hold also for lower doping, where the perturbation to the pristine dispersions is smaller. The similarity between these two models justifies our use of the rigid-band approximation to simulate substitutional doping. On the other-hand, this is the most appropriate way to account for charge transfer or gate-induced doping.

Since doping leads to a small Fermi surface centered at $\mathbf{\Gamma}$, (Fig. S1(a)), the zone-center phonons are the most sensitive to the metallic character of doped graphane. Accordingly, we carefully checked the convergence of the phonons at $\mathbf{\Gamma}$ with respect to the smearing parameter and BZ sampling at each doping level (Table S1).

Figure 1 in the main text also reports the EDOS of other 2d and 3d systems. To model bulk diamond we use a $16 \times 16 \times 16$ Monkhorst-Pack[6] mesh for BZ sampling and $1 \times 1 \times 16$ for a diamond nanowire with diameter $\sim$0.94nm. The relaxed C-C bond lengths are 1.52Å for diamond and $\sim$1.52Å (average) for the nanowire. The EDOS are calculated using the tetrahedron method[12] for BZ integration, and they are proportional to $E^{-1/2}$ in the nonowire (overlapped by van Hove singularities), a step-like function in graphane, and $E^{1/2}$

in bulk diamond, as expected for generic EDOS in systems with reduced dimensionality[13]. The step-like shape in graphane implies that the EDOS is large even at low doping.

The fundamental mechanism responsible for high-T_c in copper oxides is still debated[14–16]. Yet it is generally accepted that Coulomb exchange and correlation effects play an important role[15, 16]. However, in conventional superconductors the pairing is known to be driven by the interaction between electrons and lattice vibrations[17–26] and can be understood in the framework of the conventional BCS theory. We thus study the superconductivity of doped graphane within the isotropic approximation to the Midgal-Elashberg theory[27]. We calculate T_c using the modified McMillan equation[28] and a Coulomb parameter $\mu^\star = 0.13$ (a typical value of the Coulomb repulsion between electrons[27, 28]). Other possible choices for the Coulomb parameter do not affect our conclusions. λ and the logarithmic phonon frequencies $\omega_{\log}$ are calculated by BZ sampling on a uniform unshifted $100 \times 100 \times 1$ grid. We extensively checked the convergence of λ and $\omega_{\log}$ with respect to BZ sampling by comparing two calculations, one including $\mathbf{\Gamma}$ and another excluding it, since EPC at $\mathbf{\Gamma}$ is an integrable singularity and the total EPC depends on the BZ integration accuracy. The estimated errors arising from this singularity for a phonon grid of $100\times100\times1$ are ±0.006 for λ, $\pm0.7\text{cm}^{-1}$ for $\omega_{\log}$ and ±0.6K for T_c.

The possibility of superconductivity in alkali-doped graphene was also recently suggested[29], based on a pairing mechanism associated with an extended van Hove singularity. In hole-doped graphane, unlike alkali-doped graphene[29], E_F is located far from any van Hove singularity (see Fig. S1). Thus, the instability of Ref. 29, corresponding to an effective e-e coupling an order of magnitude smaller than the EPC here, is expected not to alter our conclusions.

PHONON DISPERSIONS

Figure S2(a) plots the phonon dispersions corresponding to the two C-H stretching modes (see Figs. S2(b,c)). These modes could be used to fingerprint graphane via IR absorption or UV Raman spectroscopy[30–32]. The C-H stretching branches are essentially unaffected by p-doping. This is consistent with the fact that the electronic states associated with the C-H bonds have negligible weight at E_F.

Figures S3(a,b) show the calculated phonon dispersions for 1% and 4% p-doped graphane.

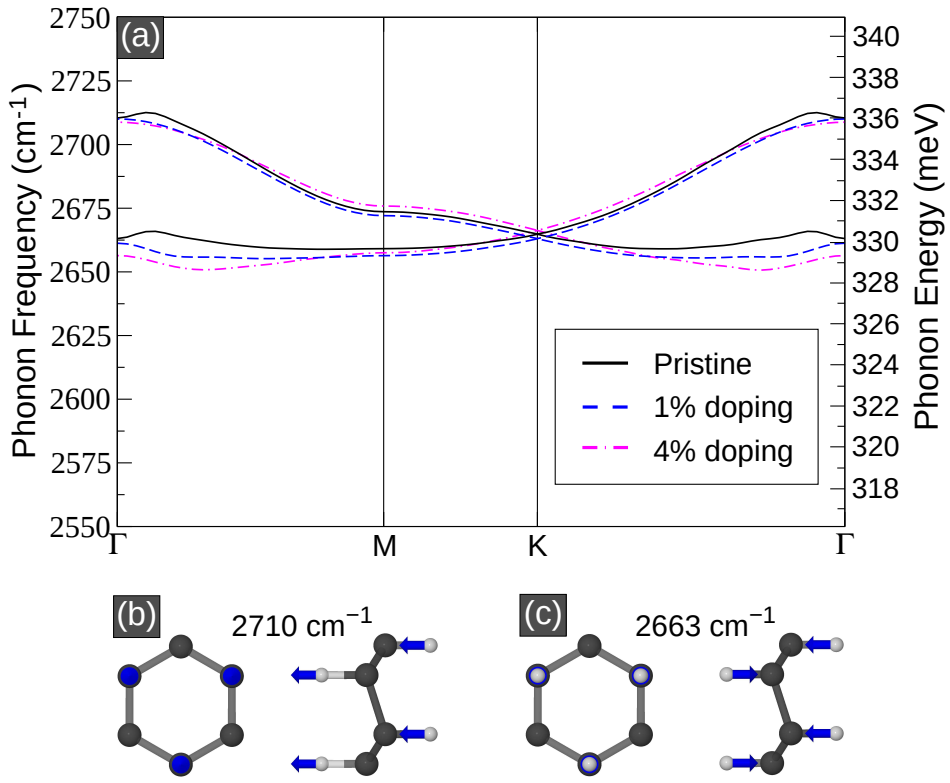

FIG. S2: (a)Dispersion of the two C-H stretching modes for pristine (solid dark lines), 1% (dashed blue lines) and 4% p-doped graphane (dashed pink lines). (b)Ball-and-stick representations of the C-H stretching motions with H atoms in phase, and (c) out of phase. The arrows indicate the H motions (C in grey, H in white)

The widths of the Kohn anomalies at $\mathbf{\Gamma}$ match the average diameter, $2k_{\mathrm{F}}$, of the hole Fermi surface at each doping level, Fig. S1(a). We note that at 4% the softening is accompanied by an hybridization of the branches leading to a level anticrossing around $2k_{\mathrm{F}}$. Figure S4 plots the displacement patterns of the optical phonon modes at each doping level. The two degenerate TO modes having planar C-C stretching and H atoms moving in-phase with the C atoms downshift from 1185 to 715cm^{-1} (147 to 89meV) for 1% doping. The phonon softening of the TO C-C stretching modes (∼58meV or ∼470cm^{-1} at 1% doping, see Table S1) is significantly larger than in other materials, as typical Kohn anomalies range from ∼5meV (graphite and graphene)[33] to ∼10meV (TaC[26]). This is due to the large EPC of the C-C bond-stretching vibration, which significantly affects the sp^3-like electronic states at the E_F. For the same doping, the two degenerate zone-centre modes having in-plane C-C stretching and H atoms moving out-of-phase with respect to the C atoms downshift from

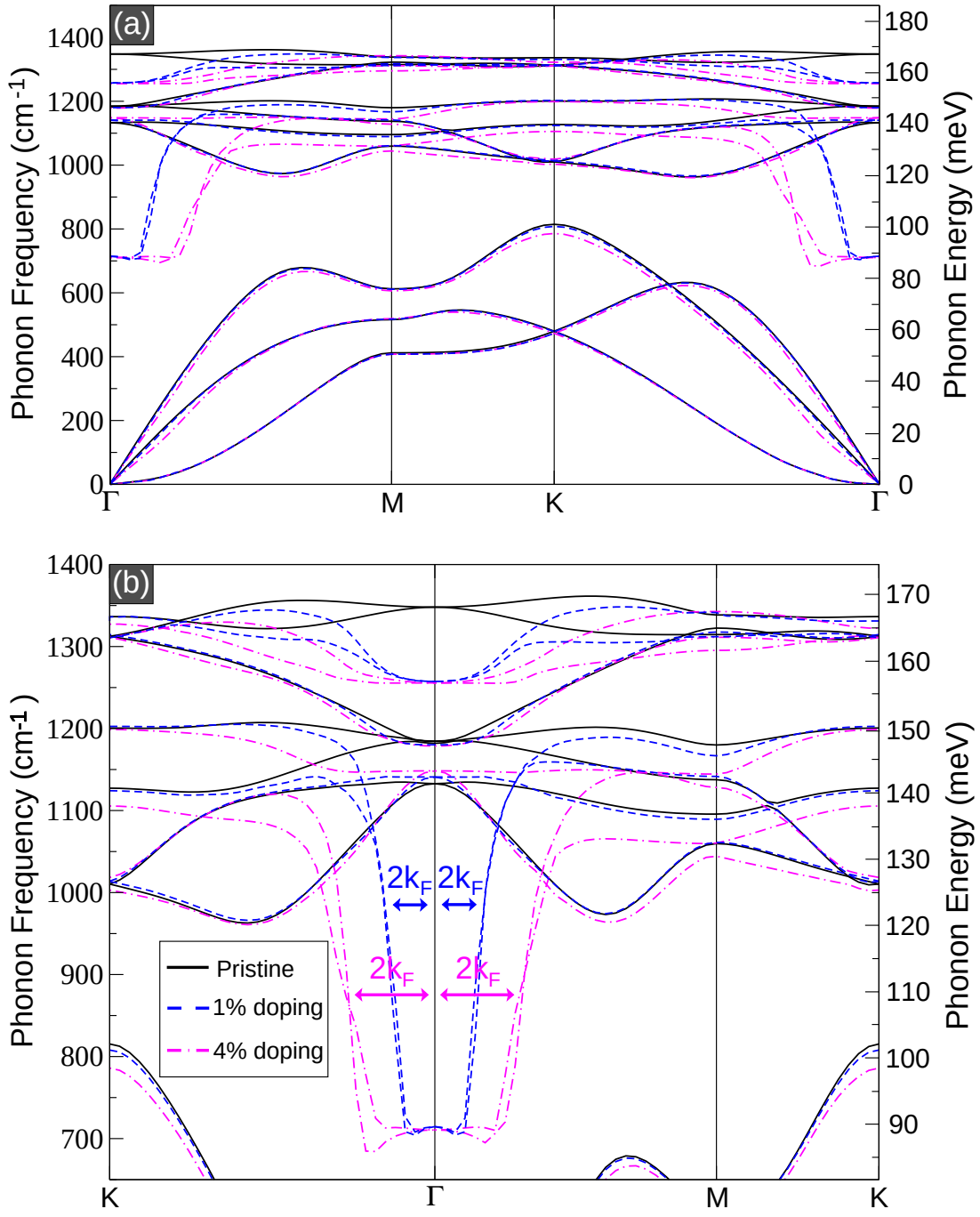

FIG. S3: (a)Phonon dispersion of pristine (solid black line), 1% (dashed blue lines) and 4% p-doped graphane (dashed pink lines). (b)Optical modes around the zone centre, showing the Kohn anomalies. Taking B explicitly into account[24], or with non-adiabatic corrections[25], may slightly revise the softening. Nevertheless, such a large softening stands out as a qualitative effect.

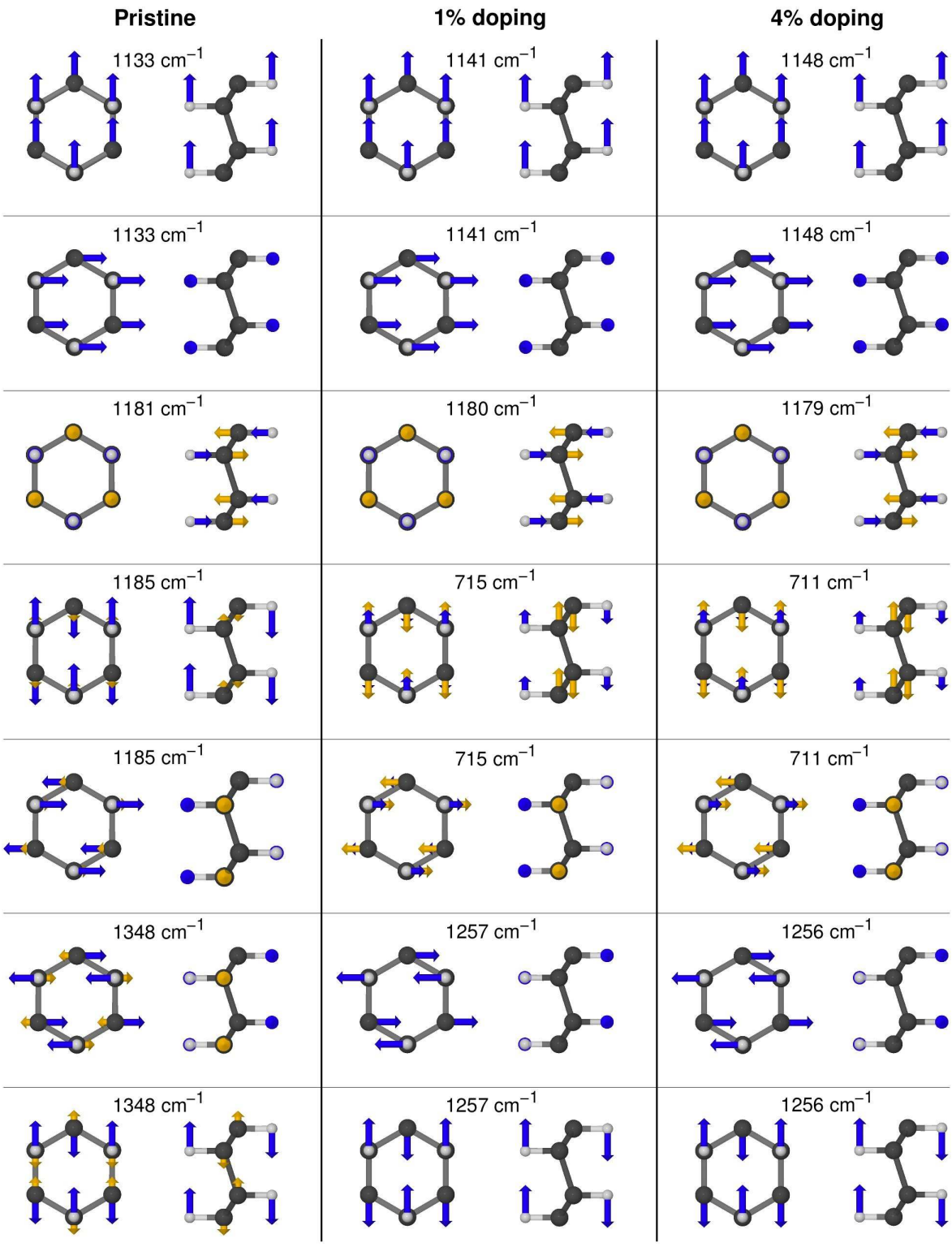

FIG. S4: Ball-and-stick representations of the optical phonon modes at $\mathbf{\Gamma}$ for (left) pristine graphane, (centre) 1% doping, (right) 4% doping. The gold (blue) arrows indicate the carbon (hydrogen) motions. Carbon atoms are shown in grey, hydrogens in white.

1348 to 1257cm^{-1} (167 to 156meV). The LO mode with out-of-plane C-C stretching does not couple to the electrons, due to the different parity of potential and wavefunctions, resulting into a vanishing EPC. The two degenerate optical modes corresponding to the shear motion of the C and H planes (at $\sim$1133cm^{-1}) and the C-H stretching modes (see Fig.S2) do not undergo softening upon doping. This is consistent with the electronic states associated with the C-H bonds having little weight at E_F, hence a small EPC.

METAL-TO-INSULATOR TRANSITION

In order to estimate the critical B doping, n_c, corresponding to the Mott metal-to-insulator transition (MIT) we use the following argument. In 3d the MIT occurs when the impurity wavefunctions are close enough that their overlap is significant[34]. For many materials $a_H n_c^{1/3} \sim 0.26$, a_H being the radius of the ground-state wavefunction of an hydrogenic donor[34]. The radius can be calculated as $a_H = \epsilon a_0/m^\star$, a_0 being the Bohr radius, ϵ the dielectric constant, and $m^\star$ the effective mass[34]. In diamond $a_H \sim 4$Å and $n_c \sim 4 \cdot 10^{20}$cm^{-3}[34], therefore the average separation between nearest neighbor B atoms is ~ 15Å. For graphane we use a similar criterion, replacing the 3d hydrogenic impurity with a 2d one. The ground-state hydrogenic wavefunction in 2d has radius $a_H^{2d} = \epsilon a_0/2m^\star$[35]. Using dielectric constant and hole effective mass of diamond ($\epsilon = 5.7$; $m^\star = 0.74$): $a_H^{2d} = a_H/2 \sim 2$Å. Thus, the average separation between nearest neighbor B atoms at MIT is ~ 7.5Å and the corresponding doping is estimated as 5% B (1 B every 20 C) or $2 \cdot 10^{14}$ holes·cm^{-2}.

[1] D. M. Ceperley,B. J. Alder, Phys. Rev. Lett. **45**, 566 (1980).

[2] J. P. Perdew, A. Zunger, Phys. Rev. B **23**, 5048 (1981).

[3] J. Ihm, A. Zunger, M. L. Cohen, J. Phys. C **12**, 4409 (1979).

[4] N. Troullier, J. L. Martins, Phys. Rev. B **43**, 1993 (1991).

[5] M. Fuchs, M. Scheffler, Comput. Phys. Commun. **119**, 67 (1999).

[6] H. J. Monkhorst, J. D. Pack, Phys. Rev. B **13**, 5188 (1976).

[7] J. O. Sofo, A. S. Chaudari, G. D. Barber, Phys. Rev. B **75**, 153401 (2007).

[8] S. Lebègue, M. Klintenberg, O. Eriksson, M. I. Katsnelson, Phys. Rev. B **79**, 245117 (2009).

[9] S. Baroni et al. Rev. Mod. Phys. **73**, 515 (2001).

[10] M. Methfessel, A. T. Paxton, Phys. Rev. B **40**, 3616 (1989).

[11] J. Noffsinger et al. Phys. Rev. B **79**, 104511 (2009).

[12] P. E. Blöchl, O. Jepsen, O. K. Andersen, Phys. Rev. B **49**, 16223 (1994).

[13] A. D. Sutton, *Electronic Structure of Materials* (Oxford Univ. Press, Oxford, 1993).

[14] J. G. Bednorz, K. A. Müller, Z. Phys. B **64**, 189 (1986).

[15] M. Tinkham, *Introduction to Superconductivity* (McGraw-Hill, New York, 1996).

[16] F. Giustino, M. L. Cohen, S. G. Louie, Nature **452**, 975 (2008).

[17] X. Blase et al. Nature Mater. **8**, 375 (2009).

[18] J. Kortus et al. Phys. Rev. Lett. **86**, 4656 (2001).

[19] K. P. Bohnen, R. Heid, B. Renker, Phys. Rev. Lett. **86**, 5771 (2001).

[20] A. Floris et al., Phys. Rev. Lett. **94**, 037004 (2005).

[21] M. Calandra, F. Mauri, Phys. Rev. Lett. **101**, 016401 (2008).

[22] K. Ishizaka et al., Phys. Rev. Lett. **98**, 047003 (2007).

[23] H. J. Choi et al. Phys. Rev. B **66**, 020513(R) (2002).

[24] X. Blase, C. Adessi, D. Connétable, Phys. Rev. Lett. **93**, 237004 (2004).

[25] A. M. Saitta et al. Phys. Rev. Lett. **100**, 226401 (2008).

[26] J. Noffsinger et al. Phys. Rev. B **77**, 180507(R) (2008).

[27] G. Grimvall, *The Electron-Phonon Interaction in Metals* (North-Holland, New York, 1981).

[28] P. B. Allen, R. C. Dynes, Phys. Rev. B **12**, 905 (1975).

[29] J. L. McChesney et al. Phys. Rev. Lett. **104**, 136803 (2010).

[30] D. C. Elias et al., Science **323**, 610 (2009).

[31] A. C. Ferrari, J. Robertson, Phys. Rev. B **64**, 075414 (2001).

[32] J. Ristein et al. J. Appl. Phys. **84**, 3836 (1998).

[33] S. Piscanec et al. Phys. Rev. Lett. **93**, 185503 (2004).

[34] E. Bustarret *et al.*, Phil. Trans. R. Soc. A **366**, 267 (2008).

[35] X. L. Yang et al. Phys. Rev. A **43**, 1186 (1991).